Pulsed/Intermittent Activation in Fusion Energy Reactor Systems

J.E. Sisolak, S.E. Spangler, D.L. Henderson

March 1992

UWFDM-882

Prepared for the 10th Topical Meeting on the Technology of Fusion Energy, 7–12 June 1992, Boston MA (Fus. Tech. 21 (May 1992) 2145.

FUSION TECHNOLOGY INSTITUTE

UNIVERSITY OF WISCONSIN

MADISON WISCONSIN

Pulsed/Intermittent Activation in Fusion Energy Reactor Systems

J.E. Sisolak, S.E. Spangler, D.L. Henderson

Fusion Technology Institute
University of Wisconsin
1500 Engineering Drive
Madison, WI 53706

http://fti.neep.wisc.edu

March 1992

UWFDM-882

Prepared for the 10th Topical Meeting on the Technology of Fusion Energy, 7–12 June 1992, Boston MA (Fus. Tech. 21 (May 1992) 2145.

PULSED/INTERMITTENT ACTIVATION IN FUSION ENERGY REACTOR SYSTEMS

J. E. SISOLAK, S. E. SPANGLER and D. L. HENDERSON
University of Wisconsin-Madison
1500 Johnson Drive Madison, Wisconsin 53706-1687
(608) 263-0808

ABSTRACT

Recently developed pulsed/intermittent irradiation calculational models were used to analyze changes in the activity of major first wall constituents (aluminum, iron, manganese) due to changes in reactor pulsing schedules. Both magnetic fusion energy (MFE) and inertial fusion energy (IFE) experimental reactor systems were considered. Comparisons among pulsing schedules with equal neutron fluences demonstrated that the activities of some nuclides can be reduced to 28% of the values computed using a baseline pulsing schedule. This can be significant if the radionuclide affected dominates the total activity of the first wall.

I. INTRODUCTION

Fusion reactor design requires the calculation of radioactivity, afterheat, biological hazard potential, and biological dose rates due to neutron activation. Such calculations help determine first wall material, maintenance procedures, blanket structure, accident analysis, and environmental impact of the fusion reactor. Current designs for magnetic fusion energy (MFE) and inertial fusion energy (IFE) reactors present a problem for the calculation of activity, since their operation is pulsed/intermittent. The problem arises in the modeling of the irradiation history for the calculation of activity and activity related parameters, such as the biological dose rate. This is particularly the case for experimental facilities, as experimental setup and maintenance require widely spaced pulses; additionally, the experimentalist and maintenance personnel would like access to the device relatively soon following a pulse. This requires a fairly accurate calculation of the biological dose rate after shutdown, which can only be obtained by modeling the irradiation history as accurately as possible. Experimental IFE devices have very short operating times ($< 1\ \mu s$) and off times ranging from minutes to severals days; experimental MFE devices are projected to operate with pulse widths ranging from several minutes to an hour and off times of several minutes.[1] In addition to the pulsed operating mode of the devices, regularly scheduled maintenance intervals, which can range from a few days to several weeks, also impose an intermittent irradiation structure on operations.

Currently several approximate methods are used to calculate the activity of fusion energy devices due to pulse/intermittent neutron irradiation. The steady state approximations are examined in the limits of very long-lived and short-lived activation products and in the limits of long and short pulse widths. The general conditions under which the approximate methods are invalid are presented and illustrate the need for a pulsed/intermittent irradiation model. The main objective of this paper is to demonstrate that the activity of a fusion energy device can be changed by altering the reactor pulsing schedule, even when the fluence is constant. We illustrate this by examining changes in the first wall activity due to variations of the basic pulsing schedule of the International Thermonuclear Experimental Reactor (ITER), a magnetic fusion energy facility, and the Target Development Facility (TDF), an inertial fusion energy experimental facility using a recently developed pulsed/intermittent calculational model. The first-wall materials are aluminum for the TDF, and iron and manganese (constituents of stainless steels) for ITER.

II. DISCUSSION OF SOLUTION METHODS

The pulsed/intermittent activation problem can be dealt with in several ways. First, it can be treated as a steady state problem in which the total operation time and total fluence are preserved. This treatment of the pulsed problem will be called the "equivalent steady state method". Unfortunately, this approximation can lead to significant errors in the calculated activity and activity related parameters.[2−4] An understanding of the magnitude of the error inherent in the equivalent steady state method can be gained by considering a simple, two nuclide chain and comparing the analytical expressions for the pulsed and equivalent steady state treatments. Figure 1 depicts an idealized series of uniformly spaced square pulses with a width of θ seconds and an "off" time (dwell time) of Δ. The neutron flux in the equivalent steady state method is related to the flux in the pulsed case as

$$\phi_{ess}\ (n\theta + (n-1)\Delta) = \phi_p\ (n\theta) \tag{1}$$

where n is the number of pulses.

The stable parent nuclide with initial concentration $N_1(0)$ and cross section σ is transmuted through a neutron interaction into a radioactive daughter nuclide N_2 with decay constant λ. We assume that the radioactive daughter nuclide is not further transmuted by neutron interactions. The ratio of the concentration of the daughter nuclide to $N_1(0)$ at the conclusion of n

pulses at a flux level of ϕ_p is given by:[5]

$$\frac{N_{2p}}{N_1(0)}=\left[\frac{\sigma\phi_p\left(e^{-\sigma\phi_p\theta}-e^{-\lambda\theta}\right)}{\lambda-\sigma\phi_p}\right]\left[\frac{e^{-n\sigma\phi_p\theta}-e^{-n\lambda(\theta+\Delta)}}{e^{-\sigma\phi_p\theta}-e^{-\lambda(\theta+\Delta)}}\right]. \quad (2)$$

The ratio of the concentration of the daughter nuclide to $N_1(0)$ for the equivalent steady state operation at a flux level ϕ_{ess} is

$$\frac{N_{2ess}}{N_1(0)}=\frac{\sigma\phi_{ess}\left(e^{-\sigma\phi_{ess}(n\theta+(n-1)\Delta)}-e^{-\lambda(n\theta+(n-1)\Delta)}\right)}{\lambda-\sigma\phi_{ess}}. \quad (3)$$

Using the relationship between ϕ_{ess} and ϕ_p in Eq. 1, the above expression becomes

$$\frac{N_{2ess}}{N_1(0)}=\frac{\sigma\phi_p n\theta\left(e^{-n\sigma\phi_p\theta}-e^{-\lambda(n\theta+(n-1)\Delta)}\right)}{(n\theta+(n-1)\Delta)\lambda-\sigma\phi_p n\theta}. \quad (4)$$

The ratio between N_{2ess} and N_{2p} at shutdown is

$$\frac{N_{2ess}}{N_{2p}}=\left[\frac{(\lambda-\sigma\phi_p)n\theta}{(n\theta+(n-1)\Delta)\lambda-\sigma\phi_p n\theta}\right]\times$$
$$\left[\frac{e^{-\sigma\phi_p\theta}-e^{-\lambda(\theta+\Delta)}}{e^{-n\sigma\phi_p\theta}-e^{-n\lambda(\theta+\Delta)}}\right]\left[\frac{e^{-n\sigma\phi_p\theta}-e^{-\lambda(n\theta+(n-1)\Delta)}}{e^{-\sigma\phi_p\theta}-e^{-\lambda\theta}}\right]. \quad (5)$$

Considering a large number of pulses ($n \gg 1$), the above equation reduces to

$$\frac{N_{2ess}}{N_{2p}}\cong\frac{(\lambda-\sigma\phi_p)\theta}{(\theta+\Delta)\lambda-\sigma\phi_p\theta}\left[\frac{e^{-\sigma\phi_p\theta}-e^{-\lambda(\theta+\Delta)}}{e^{-\sigma\phi_p\theta}-e^{-\lambda\theta}}\right]. \quad (6)$$

Several limiting cases of interest can be deduced using the relation between N_{2ess} and N_{2p} developed above.

a) For the pulse width much greater than the dwell time, that is, $\theta \gg \Delta$, Eq. 6 reduces to

$$\frac{N_{2ess}}{N_{2p}}\cong 1.$$

The equivalent steady state and the pulsed solutions yield the same result (i.e. the effect of the dwell time can be neglected).

b) For a daughter nuclide with $\Delta \gg t_{1/2}$, and $\theta \gg t_{1/2}$, and $\lambda \gg \sigma\phi_p$, Eq. 6 reduces to

$$\frac{N_{2ess}}{N_{2p}}\cong\frac{\theta}{\Delta+\theta}.$$

This implies that the equivalent steady state result will underestimate the pulsed result by a factor of $(\Delta+\theta)/\theta$ at shutdown and occurs most often for short-lived nuclides in MFE experimental devices for which the pulse width is comparable to the dwell time.

c) For a daughter nuclide with $\Delta \gg t_{1/2} \gg \theta$, and $\lambda \gg \sigma\phi_p$, Eq. 6 reduces to

$$\frac{N_{2ess}}{N_{2p}}\cong\frac{1}{\Delta\lambda}.$$

For this case the equivalent steady state result underestimates the pulsed result by a factor of $\Delta\lambda$ at shutdown. This occurs most often in IFE devices where the pulse width is considerably less than a nuclide half-life.

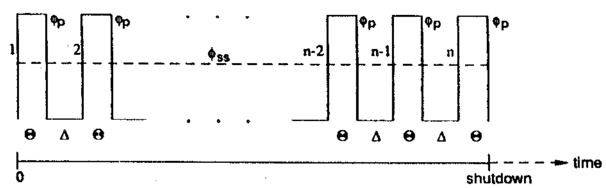

Fig. 1. Relation between the neutron flux during pulsed irradiation and the equivalent steady state flux.

d) For a daughter nuclide with $t_{1/2} \gg \Delta$, and $t_{1/2} \gg \theta$, and $\lambda \gg \sigma\phi_p$, Eq. 6 reduces to

$$\frac{N_{2ess}}{N_{2p}}\cong 1.$$

If the pulse width and dwell time are short relative to the half-life, the equivalent steady state method yields the same result as the pulsed method.

e) For a daughter nuclide with $\sigma\phi_p\theta \gg \lambda(\theta+\Delta)$, which is true for very long-lived nuclides, Eq. 6 reduces to

$$\frac{N_{2ess}}{N_{2p}}\cong 1.$$

For a very long-lived daughter, the equivalent steady state method again agrees with the pulsed method.

The above results imply that when the activity is dominated by short-lived nuclides (for which cases b and c often hold), the shutdown activity will be underestimated, which implies that all activity related parameters will also be underestimated. The dose rate results from Ref. 2-4 clearly demonstrate this for case c (IFE devices).

A second way to handle the pulsed/intermittent activation problem is as a steady state problem with the irradiation time equal to the sum of all the pulse widths and the operating flux level equal to that of the pulsed case; this will be referred to as the "steady state method". An analysis of the magnitude of the error introduced by this approximation for MFE devices has, in part, been done in Ref. 6 and will be included here for completeness and discussion purposes.

We consider the same two nuclide chain as above, with the irradiation history depicted in Fig. 1. In this approximation, the steady state neutron flux is set equal to the pulsed neutron flux, $\phi_{ss}=\phi_p$, with the steady state operation time equal to $n\theta$. The concentration of the daughter nuclide for the steady state case is

$$\frac{N_{2ess}}{N_1(0)}=\frac{\sigma\phi_p}{\lambda-\sigma\phi_p}\left[e^{-n\sigma\phi_p\theta}-e^{-n\lambda\theta}\right]. \quad (7)$$

Using Eq. 2, the ratio between N_{2ss} and N_{2p} at shutdown is

$$\frac{N_{2ss}}{N_{2p}}=\left[\frac{e^{-n\sigma\phi_p\theta}-e^{-n\lambda\theta}}{e^{-\sigma\phi_p\theta}-e^{-\lambda\theta}}\right]\left[\frac{e^{-\sigma\phi_p\theta}-e^{-\lambda(\theta+\Delta)}}{e^{-n\sigma\phi_p\theta}-e^{-n\lambda(\theta+\Delta)}}\right]. \quad (8)$$

Equation 8 gives rise to 6 limiting cases.

a) For the pulse width much greater than the dwell time, that is, $\theta \gg \Delta$, Eq. 8 reduces to

$$\frac{N_{2ss}}{N_{2p}}\cong 1.$$

The steady state and the pulsed solutions yield the same result; note that this is identical to case a for the equivalent steady state method.

b) For a daughter nuclide with $\Delta \gg t_{1/2}$, and $\theta \gg t_{1/2}$, and $\lambda \gg \sigma\phi_p$, Eq. 8 reduces to

$$\frac{N_{2ss}}{N_{2p}} \cong 1.$$

Observe that the conditions of case b for the steady state and equivalent steady state methods are the same, but the limiting results are not.

c) For a daughter nuclide with $n\theta \gg t_{1/2} \gg \theta$, and $\lambda \gg \sigma\phi_p$, Eq. 8 reduces to

$$\frac{N_{2ss}}{N_{2p}} \cong \frac{1 - e^{-\lambda(\theta+\Delta)}}{\lambda\theta}.$$

Note that for IFE devices, where the pulse width is less than $1\ \mu s$, the steady state result overestimates the pulse result considerably.

d) For a daughter nuclide with $n\theta \gg t_{1/2} \gg (\theta + \Delta)$, and $\lambda \gg \sigma\phi_p$, Eq. 8 reduces to

$$\frac{N_{2ss}}{N_{2p}} \cong \frac{\theta + \Delta}{\theta}.$$

Note that this is a further restriction of case c.

e) For a daughter nuclide with $t_{1/2} \gg n(\theta+\Delta)$, which is true for long-lived nuclides, and $\lambda \gg \sigma\phi_p$, Eq. 8 reduces to

$$\frac{N_{2ss}}{N_{2p}} \cong 1.$$

Hence when the half-life of the daughter is much longer than the total operation time of the device, the steady state approximation is valid.

f) For a daughter nuclide with $\sigma\phi_p\theta \gg \lambda(\theta + \Delta)$, which is true for very long-lived nuclides, Eq. 8 reduces to

$$\frac{N_{2ss}}{N_{2p}} \cong 1,$$

which indicates that the steady state method yields the same result as the pulsed method for very long-lived nuclides. This matches case e of the equivalent steady state method.

Equations 5 and 8 have been plotted in Figs. 2 and 3. Figure 2 employs parameters suitable for an IFE device, while Fig. 3 is representative of an MFE device. Note that for IFE devices, the equivalent steady state and the steady state approximations under-/over- estimate the pulsed result considerably for short-lived nuclides, and that the steady state model (Eq. 8) is especially poor. In Fig. 3 with Δ = 6 h, both approximations yield poor results over some range of half-lives. Equation 5 underestimates the short-lived nuclides and Eq. 8 overestimates the

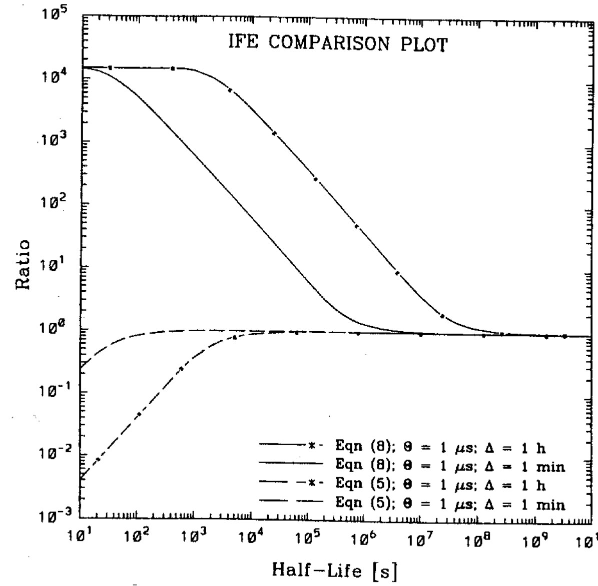

Fig. 2. IFE comparison plot.

intermediate-lived nuclides. Unfortunately nuclides with half-lives in the range from 10^3 - 10^6 seconds often strongly influence the activity in the first 6 months after shutdown. Finally, observe that in both the IFE and the MFE plots, the approximations get worse as the dwell time, Δ, increases. For both the steady state and the equivalent steady state treatments, the relation between the approximate and the exact (pulsed) results becomes complicated for nonuniform pulsing schedules or for decay chains with more than one radioactive nuclide. Figures 2 and 3, however, make clear the need for better calculational models.

A third, more realistic, treatment of the pulsed activation problem is based on the following approximation: destruction of initial and transmuted nuclides by neutron interactions in the second and subsequent pulses is ignored. That is, the approximation assumes the creation of the same amount of radioactive and stable nuclides during each pulse. Models based on this approximation have been employed in several experimental devices and reactor studies,[2−4,7−9] and produce good results provided the operating period is short, and the initial stable nuclide is transmuted to a radioactive one. Significant errors may occur for long operating times and for nuclides beyond the second in a transmutation chain.[10] Since most materials in a fusion reactor will be present throughout its lifetime and will be exposed to the total pulse history, destruction of initial and created nuclides should be taken into account in activity calculations. The final two methods discussed below satisfy this requirement.

Two calculational methods based on the linear chain method (Bateman Equations[11]) have recently been developed to compute the induced activity due to pulsed/intermittent irradiation histories.[5,10] The first method treats the case in which irradiated materials are present throughout the series of pulses. This method explicitly accounts for destruction of initial and transmuted materials during subsequent pulses, contains no approximations, and applies to any structural material in a fusion

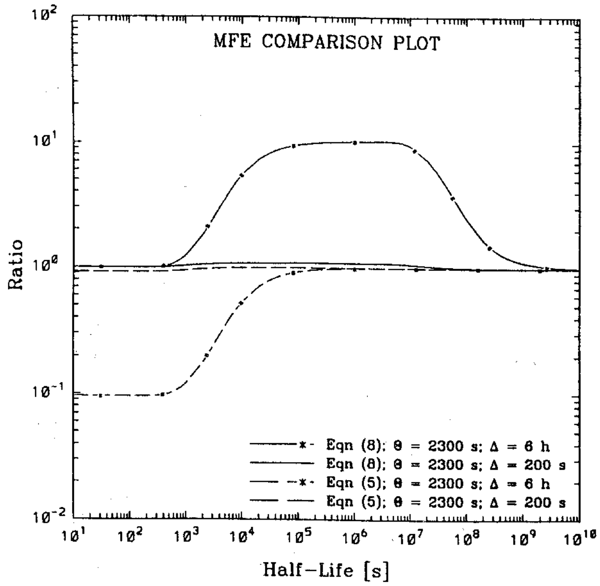

Fig. 3. MFE comparison plot.

reactor (first wall, magnet, shield, etc.) which is present in the reactor for its lifetime.

The second method handles the case in which the material concentrations are the same at the beginning of each pulse; therefore, each pulse creates a fixed amount of activated material, which is assumed to be removed prior to the next pulse. This method is exact for a recirculating fluid in a reactor which is filtered of activated materials after each pulse. It applies, for example, to recirculating coolant from which activated material is continuously extracted to reduce radiation exposure to maintenance personnel.

The methods can be combined to model irradiation histories which have characteristics of both the above cases. To see how this applies to a fusion reactor, consider a sensitive component within a reactor which requires replacement every

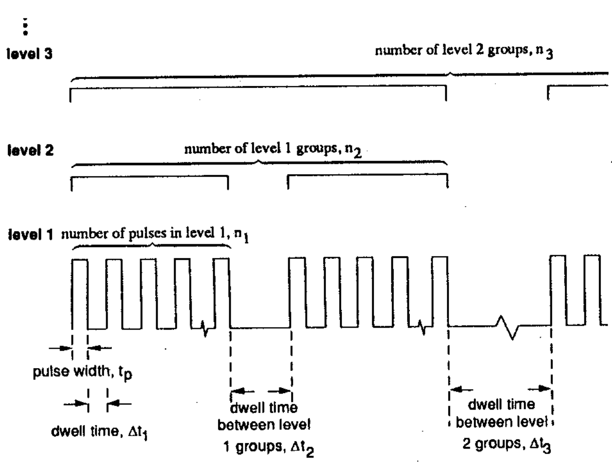

Fig. 4. Relation between various levels of regular pulse groupings during pulsed/intermittent operation.

TABLE I
Pulse Irradiation History Levels for Aluminium

	Level 1			Level 2		Level 3	
	Width t_p	Dwell Δt_1	No. n_1	Dwell Δt_2	No. n_2	Dwell Δt_3	No. n_3
1	1 μs	$\frac{2}{3}$ h	15,000	–	–	–	–
2	1 μs	1 h	15,000	–	–	–	–
3	1 μs	$\frac{2}{3}$ h	12	$16\frac{2}{3}$ h	5	$64\frac{2}{3}$ h	250
4	1 μs	1 h	12	13 h	5	61 h	250
5	1 μs	$1\frac{1}{3}$ h	12	$9\frac{1}{3}$ h	5	$57\frac{1}{3}$ h	250

6 months, due to irradiation damage. What is the total radioactivity inventory due to this component at the end of the reactor lifetime? This scenario can be modeled by applying the first method within each 6 month period, and then treating the entire 6 months as one pulse for the second method.

III. CALCULATIONAL PROCEDURE

The activation calculations were performed with a modified version of the PULSAR demonstration code[5,10] which computes the activity due to various levels of regular pulse/intermittent irradiation groups as depicted in Fig. 4. The linearized nuclide transmutation chains required for the activation calculations were obtained from the DKR-ICF radioactivity code.[12] The activation data library used by the DKR-ICF code is ACTL-LIB, which is based on the evaluated neutron activation cross-section library ACTL[13] and the Table of Isotopes.[14]

To compute the aluminum activation, the first wall neutron flux within the 1 meter radius TDF reaction chamber was employed in the DKR-ICF and subsequent PULSAR calculations. The radial build, neutron transport code, and neutron cross section library used in the TDF calculations are described in Ref. 15. The first wall flux within the inboard side of the ITER facility was used for the iron and manganese activation calculations. The preliminary neutron transport calculations required for the computation of activities were obtained from the ITER Blanket/Shield calculations.[16]

IV. RESULTS AND DISCUSSION

The pulsed/intermittent irradiation histories used for the aluminum analysis are presented in Table I, and a pictorial description of the quantities in the table and the multiple level pulsing scheme are given in Fig. 4. The irradiation histories for cases 1 and 2 consist of one level of uniformly spaced pulses, each having a pulse width of 1 μs; the dwell times between pulses are 2/3 hour for case 1, and 1 hour for case 2. The irradiation histories for cases 3 through 5 are patterned after the traditional 5 day work week, which is modeled as a 3 level irradiation scheme (see Fig. 4) in which the experimental device is operated 5 days a week for 250 weeks. Each shot consists of a 1 μs pulse and an "off" time (the level-1 dwell time); each day consists of 12 shots, followed by a night of inactivity (the level-2 dwell time); and each week consists of 5 days, followed by a weekend of inactivity (the level-3 dwell time). For cases 3, 4, and 5, the

TABLE II
Aluminum Activity Results [Bq]

Case	shutdown	1 hour	1 day	1 week	1 month
Radionuclide: Na-24, Half-life: 15 h					
1	1.56 (9)[a]	1.49 (9)	5.14 (8)	6.51 (5)	3.13 (-6)
2	1.05 (9)	1.00 (9)	3.46 (8)	4.38 (5)	2.10 (-6)
3	7.19 (8)	6.87 (8)	2.37 (8)	3.00 (5)	1.44 (-6)
4	6.66 (8)	6.35 (8)	2.19 (8)	2.77 (5)	1.33 (-6)
5	6.17 (8)	5.90 (8)	2.03 (8)	2.57 (5)	1.23 (-6)
Radionuclide: Mg-27, Half-life: 9.45 m					
1	3.55 (9)	4.38 (7)	0.00	0.00	0.00
2	3.40 (9)	4.19 (7)	0.00	0.00	0.00
3	3.55 (9)	4.38 (7)	0.00	0.00	0.00
4	3.40 (9)	4.19 (7)	0.00	0.00	0.00
5	3.37 (9)	4.15 (7)	0.00	0.00	0.00
Radionuclide: Al-26, Half-life: 7.3 (5) y					
1	5.81 (2)	5.81 (2)	5.81 (2)	5.81 (2)	5.81 (2)
2	5.81 (2)	5.81 (2)	5.81 (2)	5.81 (2)	5.81 (2)
3	5.81 (2)	5.81 (2)	5.81 (2)	5.81 (2)	5.81 (2)
4	5.81 (2)	5.81 (2)	5.81 (2)	5.81 (2)	5.81 (2)
5	5.81 (2)	5.81 (2)	5.81 (2)	5.81 (2)	5.81 (2)
Radionuclide: Al-28, Half-life: 2.24 m					
1	1.78 (9)	1.54 (1)	0.00	0.00	0.00
2	1.78 (9)	1.54 (1)	0.00	0.00	0.00
3	1.78 (9)	1.54 (1)	0.00	0.00	0.00
4	1.78 (9)	1.54 (1)	0.00	0.00	0.00
5	1.78 (9)	1.54 (1)	0.00	0.00	0.00

[a] read as: 1.56×10^9

level-2 dwell times are 40, 60, and 80 minutes, and the level-3 dwell times are 16 2/3, 13, and 9 1/3 hours. In all cases (1-5), the total number of pulses is 15,000. Since the pulse width is constant, the total neutron fluence is the same for all cases.

The results for the TDF aluminum first wall are presented in Table II. Four radionuclides, which contribute over 98% of the aluminum activity, are considered: Na-24, Mg-27, Al-26, and Al-28. They include both short-lived (Al-28) and long-lived (Al-26) radionuclides. All results are normalized to 1 cubic centimeter of solid density aluminum. The goal of the analysis is to investigate the effect of various pulsing schedules on the activity results and to explore the possibility of reducing the aluminum activity during the first week after shutdown. Note that the activity of Na-24, a major activity contributor in the first week, has been reduced by a factor of approximately 2.5 from case 1 to case 5. Since Na-24 emits fairly energetic gamma photons (2.75 and 1.37 MeV), this can be interpreted as reducing the biological dose rate attributed to Na-24 by a factor of 2.5 for a specific time after shutdown (for example, 12.5 mrem to 5 mrem at 1 week after shutdown). Given the 15 hour half-life of Na-24, it would require a waiting period of approximately 20 hours to achieve an equal reduction through decay. In addition to Na-24, major contributors to the short term activity of aluminum are Mg-27 and Al-28, both short-lived radionuclides, with half-lives of 9.45 minutes and 2.24 minutes, respectively. Due to the 40-80 minute dwell period between pulses, these radionuclides have decayed essentially to zero prior to the next pulse; hence, we note only minimal variations in the Mg-27 activity among cases 1-5. The after-shutdown activity due to these two radionuclides is effectively that which is created during the last pulse. The long term activity is dominated by Al-26. Note that for this radionuclide, as for the short-lived nuclides, the activity remains unaffected by changes in the pulsing schedule. For the pulsing schedules chosen and the total length of the operation period, the build up of Al-26 is a linear function of the total neutron fluence, so the activity remains unaffected by changes in the pulsing schedule. Thus, from the aluminum results we note that the activities of very long-lived and very short-lived radionuclides remain unaffected by changes in the pulsing schedule, whereas the activities of radionuclides with half-lives on the order of the dwell time (time between pulses) may change substantially.

TABLE III
Pulse Irradiation History Levels for Iron and Manganese

	Level 1			Level 2		Level 3	
	Width t_p	Dwell Δt_1	No. n_1	Dwell Δt_2	No. n_2	Dwell Δt_3	No. n_3
1	2300 s	200 s	50, 960	–	–	–	–
2	2300 s	786 s	140	48 h	364	–	–
3	2300 s	786 s	13	13.1 h	5	61.1 h	784
4	2300 s	1 h	13	3.70 h	5	51.7 h	784
5	600 s	360 s	50, 960	–	–	–	–

Irradiation histories for the iron and manganese components of stainless steel appear in Table III. The basic pulsing schedule for the ITER facility, consisting of 50,960 uniformly spaced pulses, constitutes case 1, for which the pulse width is 2300 seconds, and the dwell time is 200 seconds. The traditional 5 day work week is patterned in cases 2 through 4. For case 2, we increase the dwell time to 786 seconds and operate continuously for 5 days each week, while in cases 3 and 4, we reduce the number of pulses per day to 13 and vary the level-2 dwell times. Total neutron fluence is constant for cases 1 through 4, but not for case 5, in which both pulse width and dwell time are reduced.

Table IV contains activity results for the manganese stainless-steel constituent. As with the aluminum results, only the four major radionuclides are considered (Cr-55, Mn-54, Mn-56, Fe-55), since they contribute over 98% of the manganese activity. The activity results are normalized to 1 cubic centimeter of solid manganese, and, as above, the goal is to reduce the activity in the first week after shutdown by varying the irradiation history. The short-lived radionuclide, Cr-55, is not affected by changes in the pulsing schedule, as shown by the results of cases 1 through 4. A slight reduction in its activity is achieved by reducing the pulse width (case 5). This is explained by the

TABLE IV
Manganese Activity Results [Bq]

Case	shutdown	1 hour	1 day	1 week	1 month
Radionuclide: Cr-55, Half-life: 3.55 m					
1	7.02 (6)[b]	5.25 (1)	0.00	0.00	0.00
2	7.02 (6)	5.25 (1)	0.00	0.00	0.00
3	7.02 (6)	5.25 (1)	0.00	0.00	0.00
4	7.02 (6)	5.25 (1)	0.00	0.00	0.00
5	6.31 (6)	4.72 (1)	0.00	0.00	0.00
Radionuclide: Mn-54, Half-life: 312.5 d					
1	7.51 (7)	7.51 (7)	7.50 (7)	7.40 (7)	7.02 (7)
2	4.52 (7)	4.52 (7)	4.51 (7)	4.45 (7)	4.22 (7)
3	2.10 (7)	2.10 (7)	2.10 (7)	2.07 (7)	1.97 (7)
4	2.10 (7)	2.10 (7)	2.09 (7)	2.07 (7)	1.97 (7)
5	3.80 (7)	3.80 (7)	3.79 (7)	3.74 (7)	3.55 (7)
Radionuclide: Mn-56, Half-life: 2.58 h					
1	1.22 (10)	9.31 (9)	1.92 (7)	0.00	0.00
2	1.01 (10)	7.70 (9)	1.59 (7)	0.00	0.00
3	9.59 (9)	7.33 (9)	1.51 (7)	0.00	0.00
4	5.81 (9)	4.44 (9)	9.17 (6)	0.00	0.00
5	8.32 (9)	6.36 (9)	1.31 (7)	0.00	0.00
Radionuclide: Fe-55, Half-life: 2.7 y					
1	3.08 (2)	3.08 (2)	3.08 (2)	3.06 (2)	3.01 (2)
2	2.52 (2)	2.52 (2)	2.52 (2)	2.51 (2)	2.47 (2)
3	1.63 (2)	1.63 (2)	1.63 (2)	1.62 (2)	1.60 (2)
4	1.63 (2)	1.63 (2)	1.63 (2)	1.62 (2)	1.60 (2)
5	2.53 (1)	2.53 (1)	2.53 (1)	2.52 (1)	2.48 (1)

[b] read as: 7.02×10^6

fact that in cases 1-4, Cr-55 has effectively reached its saturation concentration, whereas in case 5 it has not. Since Cr-55 has a short half-life, its activity is determined primarily by the width of the last pulse: 2300 seconds (greater than 10 half-lives) for cases 1-4, and 600 seconds for case 5. Changes in the pulsing schedule do influence the activities of the other three radionuclides. The Mn-54 activity drops by a factor of 3.5 from case 1 to case 4. This reduction in the activity translates to approximately 560 days of decay time, which is significant, since Mn-54 is the dominant radionuclide 1 week after shutdown. The case 2 schedule (weekend shutdowns) produces 63% of the Mn-54 activity found in case 1, the uniformly spaced schedule. Changing the pulse width (case 5 compared to case 1) reduces the Mn-54 activity by approximately half. The Mn-56 activity, which dominates for several hours after shutdown, has been reduced by a factor of 2 from case 1 to case 4, and a change in the pulse width reduces the activity by a factor of approximately 1.4. Even larger reductions in activity are achieved for Fe-55, but it is not a dominant radionuclide, so the effects on the total activity will be negligible.

TABLE V
Iron Activity Results [Bq]

Case	shutdown	1 hour	1 day	1 week	1 month
Radionuclide: Cr-51, Half-life: 27.7 d					
1	1.00 (6)[c]	1.00 (6)	9.79 (5)	8.43 (5)	4.69 (5)
2	5.96 (5)	5.95 (5)	5.81 (5)	5.00 (5)	2.79 (5)
3	2.78 (5)	2.78 (5)	2.71 (5)	2.34 (5)	1.30 (5)
4	2.77 (5)	2.76 (5)	2.70 (5)	2.32 (5)	1.30 (5)
5	6.82 (5)	6.81 (5)	6.65 (5)	5.72 (5)	3.19 (5)
Radionuclide: Mn-54, Half-life: 312.5 d					
1	7.13 (6)	7.13 (6)	7.11 (6)	7.02 (6)	6.66 (6)
2	4.28 (6)	4.28 (6)	4.28 (6)	4.22 (6)	4.00 (6)
3	2.00 (6)	2.00 (6)	1.99 (6)	1.96 (6)	1.86 (6)
4	1.99 (6)	1.99 (6)	1.99 (6)	1.96 (6)	1.86 (6)
5	3.60 (6)	3.60 (6)	3.60 (6)	3.55 (6)	3.37 (6)
Radionuclide: Mn-56, Half-life: 2.58 h					
1	1.57 (7)	1.20 (7)	2.48 (4)	0.00	0.00
2	1.30 (7)	9.92 (6)	2.05 (4)	0.00	0.00
3	1.24 (7)	9.44 (6)	1.95 (4)	0.00	0.00
4	7.48 (6)	5.72 (6)	1.18 (4)	0.00	0.00
5	1.07 (7)	8.19 (6)	1.69 (4)	0.00	0.00
Radionuclide: Fe-55, Half-life: 2.7 y					
1	1.03 (8)	1.03 (8)	1.02 (8)	1.02 (8)	1.00 (8)
2	7.66 (7)	7.66 (7)	7.66 (7)	7.63 (7)	7.50 (7)
3	4.17 (7)	4.17 (7)	4.17 (7)	4.15 (7)	4.08 (7)
4	4.17 (7)	4.17 (7)	4.17 (7)	4.15 (7)	4.08 (7)
5	3.55 (7)	3.55 (7)	3.55 (7)	3.53 (7)	3.48 (7)
Radionuclide: Fe-59, Half-life: 44.6 d					
1	3.55 (6)	3.55 (6)	3.50 (6)	3.19 (6)	2.22 (6)
2	2.09 (6)	2.09 (6)	2.06 (6)	1.88 (6)	1.31 (6)
3	9.72 (5)	9.72 (5)	9.57 (5)	8.73 (5)	6.09 (5)
4	9.69 (5)	9.69 (5)	9.54 (5)	8.70 (5)	6.07 (5)
5	2.41 (6)	2.41 (6)	2.37 (6)	2.16 (6)	1.51 (6)

[c] read as: 1.00×10^6

Presented in Table V are the results for iron. Five radionuclides (Cr-51, Mn-54, Mn-56, Fe-55, Fe-59) produce approximately 90% of the iron activity. Since the iron pulsing schedules match those of manganese, we forgo discussion of Mn-54 and Mn-56, for which the activity variations are nearly identical to those discussed above. Cr-51 and Fe-59 both show a decrease in activity of approximately a factor of 3.6 from case 1 to case 4. Though significant, this decrease does little to reduce the total activity, due to the dominance of Fe-55. Note that in case 5, a reduction in the pulse width does not significantly reduce the Fe-59 and Cr-51 activities. For Fe-55, we see a reduction by a factor of 2.4 between cases 1 and 4; though not as drastic, this is still appreciable. Fe-55 shows a slightly greater activity reduction, a factor of 2.8 relative to case 1, when the pulse width is reduced (case 5).

V. CONCLUSION

The effect of pulsing schedule variations on the activities of several elements common in first-wall materials was examined using recently developed pulsed/intermittent irradiation models. The pulse irradiation histories used for the investigation were variations of the basic ITER and TDF pulsing schedules. For the elements and the pulsing schedules examined, reductions as high as a factor of 3.6 in the after-shutdown activity were obtained for some radionuclides. This is significant when the radionuclide dominates the total first-wall activity. The results demonstrate that the activity of very long-lived and very short-lived radionuclides remains unaffected by changes in the pulsing schedule, but the activities of radionuclides with half-lives comparable to the pulse width or the dwell time are affected. When such radionuclides dominate, the after-shutdown activity can be reduced by changing the pulsing schedule of the experimental device, even though the total neutron fluence remains constant.

VI. ACKNOWLEDGEMENTS

The authors acknowledge fruitful discussions with Dr. Mohamed Sawan, Dr. Laila El-Guebaly and Dr. Hesham Khater of the Fusion Technology Institute of the University of Wisconsin-Madison. Partial support for this work was provided by the Fusion Technology Institute.

VII. REFERENCES

1. "ITER Conceptual Design Report," ITER Documentation Series, No. 18, IAEA/ ITER/DS/18, International Atomic Energy Agency, IAEA, Vienna, (1991).

2. D.L. Henderson, M.E. Sawan and G.A. Moses, "Radiological Dose Calculations for the Diode Region of the Light Ion Fusion Target Development Facility," University if Wisconsin Fusion Technology Institute Design Memo, UWFDM-707, University of Wisconsin (October 1986).

3. H. Khater and M. Sawan, "Dose Rate Calculations for a Light Ion Beam Fusion Laboratory Microfusion Facility," Proceedings of the 13th Symposium on Fusion Engineering, Knoxville, TN, October 1989, IEEE, **2**, 1412.

4. M.E. Sawan, "Activation Analysis for the LIBRA Light Ion Beam Fusion Conceptual Design," Proceedings of the 13th Symposium on Fusion Engineering, Knoxville, TN, October 1989, IEEE, **2**, 1393.

5. S.E. Spangler, J.E. Sisolak and D.L. Henderson, "Pulsed/Intermittent Irradiation Transmutation/Activation Analysis," Document is in preparation.

6. H. Attaya, Y. Gohar and D. Smith, "US-ITER Activation Analysis," Fusion Techn., **19**, 1837 (May 1991). Paper was presented at the 9th Topical Meeting on the Technology of Fusion Energy, Oak Brook, Illinois, October 7-11, 1990.

7. R.G. Alsmiller, Jr. et al., "Dose Rates from Induced Activity in the Tokamak Fusion Test Reactor Test Cell," Nucl. Tech., **48**, 187 (1980).

8. Long-Poe Ku and J.G. Kolibal, "Radioactivation Characteristics for the Tokamak Fusion Test Reactor," Nucl. Tech./Fusion, **4**, 586 (1983).

9. R.G. Alsmiller, Jr., T.A. Gabriel and J. Barish, "Photon Dose Rate from Induced Activity in the Beam Stop of a 400 GeV Proton Accelerator," Nucl. Instru. and Methods, **155**, 399 (1978).

10. Susan E. Spangler, "A Numerical Method For Calculating Nuclide Densities in Pulse Activation Studies," Master of Science Thesis, University of Wisconsin - Madison (August 1991).

11. I. Kaplan, *Nuclear Physics* (Addison-Wesley Publishing Company, Inc. 1963).

12. D.L. Henderson and O. Yasar, "DKRICF: A Radioactivity and Dose Rate Calculation Code Package," UWFDM-714, University of Wisconsin Fusion Technology Institute, Vol. 1, Madison, Wisconsin (1986).

13. M.A. Gardner and R.J. Howerton, "ACTL: Evaluated Neutron, Activation Cross Section Library - Evaluation Techniques and Reaction Index," UCRL-50400, **18** (1978).

14. C.M. Lederer et al., *Table of Isotopes*, Sixth and Seventh Editions, Wiley (1967 and 1978).

15. O. Yasar, M.E. Sawan, D.L. Henderson and G.A. Moses, "Radiological Dose Calculations for the Chamber and Diode Region of the Light Ion Fusion Target Development Facility," Proceedings of the 12th Symposium on Engineering Problems of Fusion Research, Monterey, California, October 1987, IEEE, Catalog No. 87CH2507-2, **2**, 877.

16. L.A. El-Guebaly and M.E. Sawan, "Shielding Considerations for ITER: Current Status and Future Directions," To be presented at the New Horizons in Radiation Protection and Shielding meeting, April 26 - May 1, 1992 in Pasco, Washington.